Reinforced Plastics
ISSN (online): 0034-3617

Performance Enhancement in Silicon Solar Cells: A Systematic Analysis of MgF^2, SiO^2, and TiO^2 Coatings

Nawfal A. Saiwan
Shahid Chamran University
nawfaldiwan@gmail.com

Abstract

The conversion of power efficiency, or PCE, is the main metric used to evaluate the performance characteristics of solar cells. The anti-reflective coating (ARC) increases the power conversion efficiency (PCE) of solar cells by preventing light loss on their surface. This study investigates the different materials applied as double-layer anti-reflective coatings (DLARC) on crystalline silicon (c-Si) solar cells. The complete procedural process for silicon solar cell simulation was performed using PV Lighthouse's Wafer Ray Tracer application. Examined were five light trapping (LT) methods with various kinds of double layers. In comparison to the reference c-Si (without ARC), the highest potential photocurrent density (Jmax) of c-Si with ARC shows an improvement. At 42.20 mA/cm2, SiO2/TiO2 yields the highest value of Jmax in LT S II. Structure II's Jmax improvement was the highest, at 10.01%. According to this finding, DLARC may be utilized to reduce optical loss and raise solar cell efficiency.

Specific contribution

This study contribute to the body of knowledge on the field of solar cell surface coating with anti-reflective substance. Comparing double layer antireflection coating to single layer antireflection coating, it was discovered that the latter may greatly lower reflectance over a broad range of wavelengths. An appropriately designed double layer antireflection coating can significantly increase solar cell efficiency. The study also makes clear how various components interact to improve solar cell performance. The utilization of crystalline silicon (c-Si) solar cells and Wafer Ray Tracers application makes this research novel.

1.0 Introduction

Nowadays, solar energy is the most promising energy source available. One major benefit of solar cells over conventional power generation systems is their ability to instantly transform sunlight into solar energy. Cells using two different layers of semiconducting material, p-type and n-type material, make up modern photovoltaic technology. The electron receives energy from the photon and travels from a single layer to the next when it strikes this combination of materials with the appropriate energy. As a renewable energy source, solar cell development has accelerated significantly in the last several years. The installation of solar photovoltaic (PV) capacity is outpacing that of other generation technologies, according to global statistics. A photon's energy is absorbed by an electron, which then raises in energy when it collides with particular materials to produce electricity. In contemporary technologies, this phenomena is used in the manufacture of solar cells.[1-3].

For light to be converted into electricity, solar cell efficiency is essential [4-6]. Analyzing the amount of current a solar cell produces is one technique to gauge its efficiency. Therefore, the transmission, reflection, and absorption of light when it hits the solar cell surface are the key elements influencing the efficiency of a solar cell conversion system. Presently, the average efficiency of solar cells is around 15% [7, 8], which means that approximately 85% of incident light is not converted into usable power by the solar cell. To increase the amount of light absorbed by the solar cell surface, anti-reflective coating (ARC) materials can be applied to the cell.

This will help to resolve the issues. For solar cells to increase light trapping and reduce light reflection, their surface must be texturized [9].

Spreading aligned pyramid structures with upward points over the surface is the most common texturing technique for monocrystalline silicon wafers. This is accomplished by pointing upward from the front surface and etching. A number of experiments were carried out, including the addition of ARCs, to reduce cell reflections. ARCs are necessary for the cover glass of the solar cell. An ARC is now present on the cover glass or solar cell with more than 70% of PV panels that are sold. The idea behind anti-reflection coatings is that a thin film forms a twofold contact, which produces two reflected waves.

Literature Review

Established in 1964 [10,11], the first ARC was launched. Single layer anti-reflective coatings, or SLARCs, are frequently applied to industrial solar cells [12].

A SLARC can achieve an efficiency of roughly 16–20% on planar surfaces with a surface reflection of less than 10%, according to prior research [13–17]. A SLARC can reduce surface reflection to nearly nil at a single wavelength, depending on the materials and thickness [12,18,19]. Due to special characteristics like surface and bulk passivation, a set design of coatings is much desired to attain a greater efficiency since it lowers the overall reflection throughout a larger spectrum [18,20]. A double layer anti-reflective coating (DLARC) can reduce reflection over a wider spectrum by taking use of the phenomenon known as destructive interference of waves [13,15,16,21].

Multi-layer anti-reflective coatings can even produce higher passivation properties and have less reflections across a wider range spectrum when compared to SLARC and DLARC [12,13,18]. Applying multi-layer anti-reflective coatings is challenging, nonetheless, since coating design necessitates complicated equations and adhesion issues. Furthermore, prior research has demonstrated that coatings on textured surfaces can further minimize surface reflection [12]. Multiple-layered coatings can lessen apparent range loss [22].

The amount of light that an object reflects off its surface depends on its refractive index. The surface's density, or refractive index, should be as near to that of air as feasible in order to reduce reflection [3]. The three most widely utilized materials are titania (refractive index: 2.3), aluminum (1.65), and silica (1.45) among others. It is noteworthy that magnesium fluoride has a refractive index of 1.37 as well, despite not being used extensively. The number of coating layers is a crucial factor to take into account while producing antireflective films. One can create single-, double-, and multi-layer antireflection coatings. Generally, anti-reflective materials used in solar cells are single-layer coatings with a thickness equal to one-fourth of the wavelength of incident light. While single layer coatings are non-reflective at only one wavelength, numerous attempts have been made to enhance antireflection coatings in order to produce multilayer thin films.
For broader wavelengths, two- and multi-layer coatings are employed to address problems including increased light transmission.

The thickness of each layer in two-layer coatings can be one-fourth or half of the wavelength of the incident light, and they show a V-shaped transmission curve. These coatings can achieve up to 99% light transmission [5]. One material with distinct structures for each layer can be used in two-layer and multi-layer coatings, or separate materials can be used. For example, two-layer coatings of SiO_2 and ZrO_2 lower the refractive index over a larger wavelength range [6]. Moreover, TiO2 single-layer, SiO2/TiO2 two-layer, and SiO2/SiO2-TiO2/TiO2 multi-layer coatings have all been applied on single-crystal solar cells with success via spinning [7].

The tetragonal crystal structure of magnesium fluoride (MgF2) comes with a molar mass of 62.3018 g/mol. The chemical compound silica, or SiO2, has a molar mass of 60.1 g/mol and a tetrahedral structure. The hydrophilic three-layer silica antireflective coating mentioned above was developed to provide anti-fog properties and achieved 98% transmission, as reported by Xin Du et al. [8]. Remache et al. coated a silicon solar cell with a silica antireflective material, resulting in a 9% increase in the solar cell's productivity [9]

One of the most commonly used materials for anti-reflection coatings is magnesium fluoride (MgF_2) due to its low refractive index. When using MgF_2, it is preferable to use a substrate with a high reflection index, such as ZrO_2, SiO_2, etc., especially when combined with TiO_2. TiO_2 thin films, if made thin enough, have good reflectivity across a wide spectrum (up to 10-12 m), making them suitable for use in the production of dielectric multilayer mirrors. The reflection coefficient of TiO_2 has been reported to range from 1.9 to 2.6, depending on the substrate temperature, oxygen partial pressure, and deposition technique.

In particular, titanium dioxide (TiO_2) exhibits different phases at various temperatures, and the crystallographic orientation in which it grows impacts the refractive index. Taking these factors into account, all quarter wave (/4, = 550nm) layers of magnesium fluoride (MgF_2) and titanium dioxide (TiO_2) were deposited under ideal coating conditions in this experimental study. These ideal conditions were determined through several studies on deposition rate, substrate temperature, pressure, and other factors. For example, a single layer anti-reflective coating made of magnesium fluoride (MgF_2) would have a reflectivity of about 2% at 550 nm, while a multilayer coating designed for the same center wavelength of 550 nm might have a reflectivity of 0.2%.[7.9].

Many techniques, such as sputtering [10], pulsed laser deposition [11], chemical vapor deposition [12], chemical bath deposition [13], photochemical deposition [14], pulsed electrochemical deposition [15], and electron gun [16, 17], can be used to deposit

silica and magnesium fluoride. Dense and porous coatings are produced using these techniques [18]. Radiofrequency (RF) magnetron sputtering is regarded as one of the most effective techniques for thin-film preparation. By regulating the development conditions of the layers, this technique ensures homogeneous and uniform deposition.

Furthermore, because the coating is applied in a plasma environment, the substrate's surface is thoroughly cleaned and roughened, improving adherence.

The research aimed to observe the impact of different types of double layer antireflection coatings (DLARC) with optimal refractive index on the maximum power photocurrent density (Jmax) for silicon solar cells. By studying the effects of various DLARC types, the goal was to determine the best conditions for increasing the power photocurrent density for silicon solar cells [23]. The research also aimed to enhance our understanding of the optical and electrical properties of silicon solar cells by using different forms of DLARC. It was found that double layer antireflection coating can significantly reduce reflectance across a wide range of wavelengths compared to single layer antireflection coating. Properly constructed double layer antireflection coating can greatly improve the performance of solar cells. Additionally, the study clarifies how different elements work together to enhance solar cell performance.

Research aim and Objectives

The research aimed to observe the impact of different types of double layer antireflection coatings (DLARC) with optimal refractive index on the maximum power photocurrent density (Jmax) for silicon solar cells. By studying the effects of various DLARC types, the goal was to determine the best conditions for increasing the power photocurrent density for silicon solar cells [23]. The research also aimed to enhance our understanding of the optical and electrical properties of silicon solar cells by using different forms of DLARC. It was found that double layer antireflection coating can significantly reduce reflectance across a wide range of wavelengths compared to single layer antireflection coating. Properly constructed double layer antireflection coating can greatly improve the performance of solar cells. Additionally, the study clarifies how different elements work together to enhance solar cell performance.

The objectives are hereby highlighted;

a. To observe the impact of different types of double layer antireflection coatings (DLARC) with optimal refractive index on the maximum power photocurrent density (Jmax) for silicon solar cells.
b. To determine the best conditions for increasing the power photocurrent density for silicon solar cells
c. To enhance our understanding of the optical and electrical properties of silicon solar cells by using different forms of DLARC.

Hence, the research questions are as stated ;

a. What is the impact of different types of double layer antireflection coatings (DLARC) with optimal refractive index on the maximum power photocurrent density (Jmax) for silicon solar cells?.

b. At what best conditions suitable for increasing the power photocurrent density for silicon solar cells?

c. What are the understanding of the optical and electrical properties of silicon solar cells by using different forms of DLARC?

2.0 Research Methods (Experimental)

2.1 Simulation Design

The Wafer Ray Tracer software from PV Lighthouse is utilized to simulate a silicon solar cell using a comprehensive process approach. This modeling simulation tool is chosen for its ability to save time, money, and effort in analyzing the impact of altering the solar cell configuration. The upcoming investigation may involve using an experimental laboratory technique once the crucial parameters have been identified. The proposed experimental design schematic diagram for thin crystalline silicon (c-Si) with upright pyramid surface texturing and double layer ARC is depicted in Fig. 1.

A random upright pyramid with a 54.74-degree angle, a height of 3.54 μm, and a width of 5 μm is the configuration of the pyramid surface morphology. In order to achieve high photocurrent density and photoelectric conversion efficiency, ultrathin c-Si solar cells—whose thickness is 200 μm is needed to minimize their absorbance of light. This is a creation and modelling of an upright pyramid surface texturing using double-layer ARC and ultrathin c-Si cells. Table 1 displays each of the constant variables for the reflected light used in the simulation.

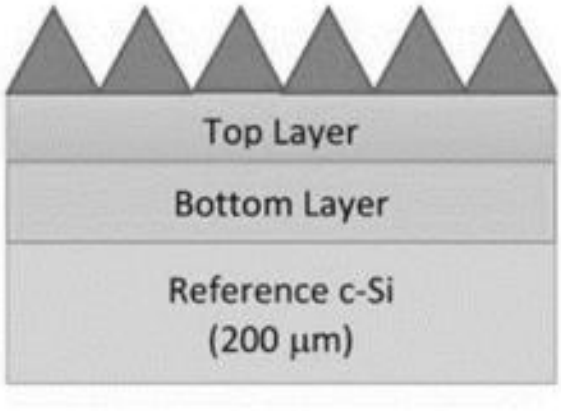

Figure 1. Schematic picture of thin C-Si with surface texturing of double layer ARC.

Table 1. Incident Light in constant variables simulation

Variables	Values
Incidence angle Θ	0℃
Spectrum	AMI.5G Sunlight
Wavelength (Min)	300nm
Wavelength(Max)	20nm
Total number of ray in a run	5,000
Optimal rays (max.)	50,000

The schematic structure diagram for the solar cell's light-trapping technique is shown in Fig. 2(a)–(f). The layout of silicon solar cells with no anti-reflective coatings is shown in Fig. 2(a), which will serve as a guide. Fig. 2(b)–(f) will include bilayer anti-reflective coatings incorporated into the system. Every substrate crystalline silicon has the same thickness, which is 200 µm. In the meantime, 75 nm thick layers of DLARC were applied, to reduce reflection at 600 nm wavelength [24]. Various DLARC material types were suggested, as Fig. 2 below illustrates.

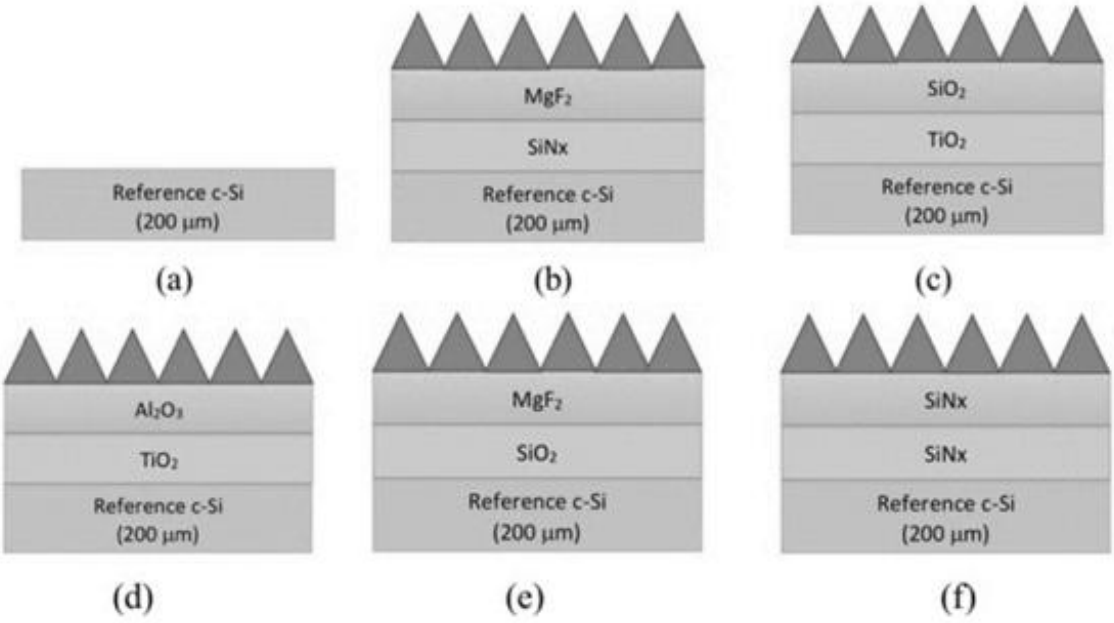

Figure 2.The Light Trapping Reference Structure is shown in Figure 2(a). Structure I: MgF_2/SiNx (c) DLARC-equipped silicon solar cell Structure II: SiO_2/TiO_2 DLARC silicon solar cell (d) Structure III: Al_2O_3/TiO_2 DLARC-equipped silicon solar cell (e) Structure IV: MgF_2/SiO_2 DLARC-equipped silicon solar cell (f) Scheme V: DLARC of SiNx/SiNx silicon solar cell.

Data Collection and Analysis

Low refractive index materials are typically employed for the top layer of a DLARC, while high refractive index materials are favoured for the bottom layer due to their important function in lowering the reflectance of incident light [25]. Table 2 displayed the ideal refractive index values for the 75 nm thickness of each top and bottom layer ARC on the silicon surface (air/top ARC/bottom ARC/Si structure, for $_{\gamma}$ = 600 nm).

Result 1

Table 2 Refractive Index values

I.T	ARC Layer		Refractive Index, ITARC		Ref.
	Layer at top	Layer at bottom	Layer at top	Layer at bottom	
Ref. Structure	Not coated	Not coated	-	-	-
Structure I	MgF_2	SiNx	1.39	1.92	[26]
Structure II	SiO_2	TiO_2	1.45	2.33	[27]
Structure III	Al_2O_2	TiO_2	1.63	2.33	[28]
Structure IV	Mg F_2	SiO_2	1.39	1.47	[29]
Structure V	SiNx	SiNx	1.92	1.92	[30]

Data Collection and Analysis 2

2.2 Photocurrent density (Jmax)

This simulation plots the transmission, absorption, and reflection gains. Jmax is a measure of the absorption result in a solar cell under particular conditions, resulting in the photocurrent maximum density. Jmax is computed by integrating the absorption curve for wavelengths ranging from 300 to 1200 nm in the AM1.5 solar spectrums [31]. Jmax is determined using Eq. (1) [32].

$$J_{max} = q \int_{300\ nm}^{1200\ nm} EQE(\lambda).S(\lambda)d\lambda \quad \text{.....(1)}$$

Where s ($_{\gamma}$) is the typical sunlight spectral photon density for the AM1,5G spectrum, and q is the electron charge. In this computation, the carrier absorption is taken to be 1 (I,e, internal quantum, IQE = 1).

3.0 Findings and Discussion

Discussion 1

3.1 Reflection, Absorption, and Transmission Comparison Curve

The primary goal of ARC is to lessen the optical losses brought on by the solar cell, as was indicated in the preceding section. When light enters a solar cell, many optical phenomena can occur. This research paper focuses on three primary optical properties: transmission, absorption, and reflectance. Since it doesn't produce energy, light that is reflected back into the atmosphere cannot be used in solar cells. As a result, it's critical to reduce reflection and boost absorption in solar cells. The accompanying figures below show the curves for transmission, absorption, and reflection for a 200 μm silicon solar cell. Analyzing the reference graph allows for a comparison of the variations amongst the five distinct LT systems. To see the variations, the reference graphs for transmission, absorption, and reflection are closely examined. All of the graphs' wavelengths fall between 300 and 1200 nm.

The reference curve with no anti-reflective coating has the most prominent reflection curves, as shown in Fig. 3(a).
Structure I, which shows the trend when DLARC of MgF2/SiNx were introduced, shows a minor drop at first, subsequent to a slight rise in the 300–400 nm range. This implies that there may have been a slight variation in the reflection values over this wavelength range. From 400 nm to 1000 nm, it then becomes comparatively steady, showing a continuous pattern. Nevertheless,

there is a discernible change in the trend after 1000 nm. The graph abruptly starts to rise sharply, suggesting that the reflection value has risen significantly.

Nearly identical reflection curve patterns are seen for Structure I, Structure II, Structure III, Structure IV, and Structure V. Despite the fact that the schemes employed various kinds of DLARC, this scheme modification is comparable. Nevertheless, Structures III and V, have a small variation from other structure reflection curves at a certain location. The reflection curves in Structure V get steeper from 400 to 500 nm. The curve begins to decline and stays that way until the wavelength reaches 1000 nm. Due to the low refractive index between the top and bottom layers of ARC, the SiNx DLARC cannot successfully perform anti-reflection in the short waveband, which results in low passivation effect [33]. As a result, this reflection displays a different curve than other structure.

In the meantime, the absorption curve (Fig. 3(b)) is slightly lower in the 300–400 nm region and briefly increases in comparison to the reference absorption curve. The curve begins to incline around 400 nm and stays consistent until 500 nm. At the curve's end, the curve then sharply declines. The reference silicon solar cell absorbs sunlight more effectively when DLARC is introduced. This is as a result of DLARC having a higher absorption value than an uncoated solar cell. While the reference curve only reaches 0.9 absorption value as the greatest value, all DLARC schemes have the same highest absorption value of 1.0.

The DLARC and reference solar cell curve patterns are identical to the reference curve, with minor variations at specific points within the design. In comparison to other structure, the absorption for structures II and III is lowest at 300 nm. After reaching 400 nm, the absorption of both structure increases sharply from 0.1 at 300 nm. Scheme IV, on the other hand, begins at 300 nm with the maximum absorption value of 0.8. The absorption patterns matched those of earlier research [25–31, 33].

Finally, the silicon solar cell transmission curve is shown in Fig. 3(c). Both DLARC and uncoated follow the same curve pattern. Every transmission curve in the graph, which spans the wavelength range of 300 nm to 1000 nm, displays a single value at all times. After that, the curves start to significantly rise above 1000 nm.
Structure V's transmission curve lies in the lowest range, between 1100 and 1200 nm. This indicates that the poorest solar cell transmission is found in the DLARC of SiNx/SiNx. Refractive indices may have an impact on transmittance. For instance, a high transmittance of 97.1% is obtained with an index of refraction in the range of 1.25–1.27. On the other hand, silicon-based materials possess a refractive index greater above those of 1.89–3.02 [34, 35].

Result 2

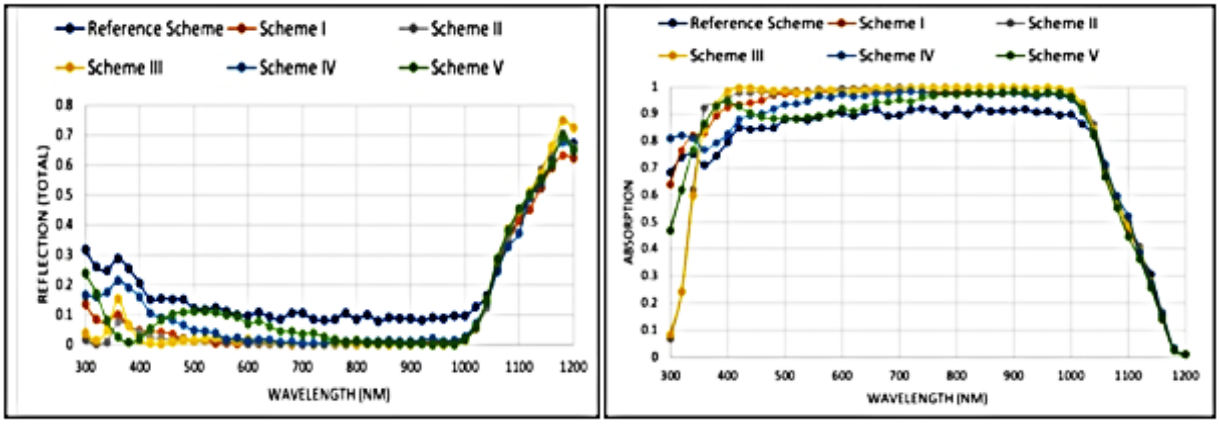

(a) (b)

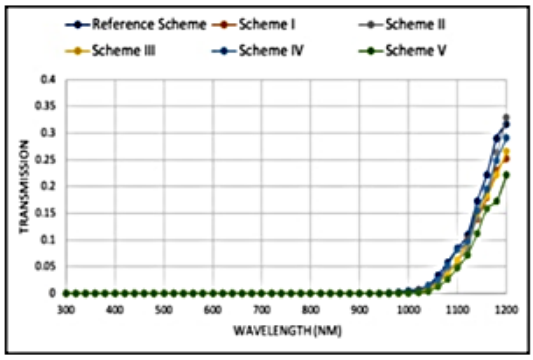

(c)

Results graph of the LT structure (a) Reflection (b) Absorption (c) Transmission curves for thin c-Si (200 mm thickness) with various DLARC types (Al2O3/TiO2), (MgF2/SiO2), (MgF2/SiNx), and (SiNx/SiNx). Moreover, the reference structure (blue curve) has been included for contrast.

NOTE: Scheme was used in the analysis software system for logistics reason, hence, it represent the structures samples as already been indicated in the content of this write up. Hence, structure I indicate scheme I in the figure, Structure II indicate scheme II, Structure III indicate scheme III,Structure IV indicate scheme IV and Structure V indicate scheme V..

Discussion 2

3.2 Maximum Current Density and the Impact of Various Anti-Reflective Coating Types

The Jmax value for a Si solar cell with a 200 m thickness utilizing LT techniques is shown in Table 3 below.

The aim of the research was to identify the optimal DLARC architecture for optimizing Jmax. Comparing the Jmax readings derived from various anti-reflective coatings to an uncoated reference Si solar cell allowed for the evaluation of the efficiency increase provided by each anti-reflective coating. The objective was to identify the anti-reflective coating with the highest Jmax, an indicator of its superior capacity to raise the existing density of the solar cell. Jmax is 38.36 mA/cm2 for the reference Si solar cell with no ARC.

Structure I's Jmax value is higher than that of the c-Si reference. Additionally, there was a rise in incident photon absorption as indicated by the value of Jmax enhancement, which increased by almost 8.13%. This demonstrates how well a two layer anti-reflective coating works to minimize reflections and increase incident photon absorbance. Next, the SiO2/TiO2 (Scheme II) Jmax value is 42.20 mA/cm2, and the Jmax enhancement indicates an increase of up to 10.01%. Comparing Scheme II to other schemes, its Jmax value is the greatest. This demonstrates how Structure II's mix of desirable material qualities results in an effective output. Moreover, Structure III has a Jmax boost of 9.65% and a Jmax value of 42.06 mA/cm2. In comparison to Structure II, the value has somewhat decreased.

Subsequently, structure IV (MgF2/SiO2) has a Jmax value of 40.88 mA/cm2 and a Jmax improvement of 6.57%. This value reduces more than Structures II and III. Lastly, Structure V has a Jmax value of 40.04 mA/cm2, which is the the lowest among the remaining structures yet remains higher than reference c-Si. The Jmax improvement decreased by approximately 4.38% relative to other structures, indicating that this particular structure is less effective in transforming incoming light into electricity. Based on Table 3, Structures II and III exhibit superior Jmax efficiency in comparison to other structures. The Jmax value may be affected by the characteristics of the material. in which it is able to absorb photon occurrence and convey it more efficiently.

A high Jmax value indicates excellent light-to-power conversion performance from a solar cell. To achieve a high Jmax, a number of components must come together. For example, the solar cell needs to efficiently collect a great deal light as achievable, prevent losses from charge carrier recombination, reduce resistance in the connections to the electricity, and make sure that charges flow through the circuit without any problems. µ

Due to its direct correlation with the solar cell's power output, a high Jmax value is essential. A higher current density can enhance the solar cell's performance in general and boost its ability to convert sunlight into useful energy by producing greater amounts of electricity.

Table 3 summarizes the Jmax readings for Si solar cells with 200µm wavelengths spanning 200 and 1200 nm, based on LT structure. Citation For the sake of comparing the LT structures, a Si solar cell with no ARC is presented.

I.T Structure	Jmax (mA/cm3)	Jmax (Enhancement Percentage)	Ref
Reference Structures(200µ thickness and no ARC)	38.25	-	-
Structure I: MgF_2 /SiNx ARC	41.37	8.12	[26]
Structure II: SiO_2/TiO_2 ARC	42.22	10.10	[27]
Structure III: Al_2O_3/TiO ARC	42.05	9.64	[28]
Structure IV: MgF_2/SiO_2ARC	40.78	6.56	[29]
Structure V: SiNx/SiNx ARC	40.03	4.37	[30]

Structure II, which had the greatest Jmax of 42.20 mA/cm^2, had been treated using titanium dioxide (TiO^2) for the DLARC and silicon dioxide (SiO_2) for the low-index. Since TiO_2 has a higher refractive index than the medium it surrounds and less loss of reflection at the surface, it exhibits enhanced Jmax efficiency [36, 37]. SiO^2, which functions as the low-index material and further reduces reflection, enables a smooth transition between the TiO^2 layer and the substrate. These findings are also consistent with earlier studies conducted by Rathanasamy et al., 2022 [27].

TiO_2 has many desirable qualities that make it an excellent material for antireflection coating in photovoltaics, including a compatible refractive index, resilience, stability, toughness, and strong resistance to force and transmittance [38]. Using an amalgamation of Al_2O_2/TiO_2 as DLARC substances, Structure III produced the second-highest Jmax (42.06 mA/cm2). In terms of refractive index, the combined effect of the materials is comparable to Scheme II, with a little variation across the top and bottom layers of ARC (see Table 2).

This means that, in comparison to other structure, Structure II and III exhibit good Jmax augmentation since the two-layer structure contains TiO_2 as one of its constituents. As for Structure V, it yields the lowest Jmax when compared to other structure because it uses ARC SiNx/SiNx. As anticipated, a blend of SiNx/SiNx with a comparable thickness and refractive index was unable to efficiently reduce light reflection, which resulted in low absorption.

4.0 Conclusions and Recommendation

The simulation structure using Wafer Ray Tracer had shown;

That Structure II: with DLARC SiO_2/TiO_2 generates the greatest value of Jmax at 42.20 mA/cm_2. This suggests that Structure II had the highest Jmax improvement, at a value of 10.01%.

This finding implies that DLARC may be used to improve the performance of solar cell applications through lowering surface reflectance and improving the absorption of incident light.

It was found that double layer antireflection coating can significantly reduce reflectance across a wide range of wavelengths compared to single layer antireflection coating. Properly constructed double layer antireflection coating can greatly improve the performance of solar cells. Additionally, the study clarifies how different elements work together to enhance solar cell performance.

In conclusion, multi-layer, double-layered anti-reflective coatings have significant impacts on the solar cell industry, improving solar energy conversion efficacy and efficiency.

Based on the aforementioned, the results of the simulation and the findings show that the goal of the study has been achieved. Finally, but just as importantly, it can be recommended that scientists can take the information gleaned from simulations and apply it to actual laboratory trials.

References

[1] A. Blakers, Solar is now the most popular form of New Electricity Generation Worldwide. The Conversation, 2023.
[2] M. Victoria, N. Haegel, I.M. Peters, R. Sinton, A. Jager-Waldau, C. del Canizo, et al., Joule. 5 (2021) 1041-1056.
[3] D. Gielen, F. Boshell, D. Saygin, M.D. Bazilian, N. Wagner, R. Gorini, Energy Strategy Rev. 24 (2019) 38-50.
[4] Y. Seekaew, O. Arayawut, K. Timsorn, C. Wongchoosuk, Carbon-Based Nanofillers and Their Rubber Nanocomposites. (2019) 259–283.
[5] F. Dincer, M. Meral, Smart Grid and Renewable Energy. 1 (2019) 47-50.
[6] A.S. Al-Ezzi, M.N.M. Ansari, Applied System Innovation. 5 (2022) 67.
[7] J. Marsh, Energysage, 2023.
[8] M.A Green, E.D. Dunlop, J. Hohl-Ebinger, et al., Prog Photovolt Res Appl. 30 (2022) 687- 701.
[9] J. Kim, D. Inns, K. Fogel, D.K. Sadana, Solar Energy Materials and Solar Cells. 94 (2010) 2091–2093.
[10] A.S. Sarkın, N. Ekren, S. Sağlam, Solar Energy. 199 (2020) 63–73.
[11] C.R. Nave, Anti-Reflection Coatings, 2017.
[12] N. Sahouane, A. Zerga, Energy Procedia. 44 (2014) 118-125.
[13] G.F. Zheng, S.R. Wenham, M.A. Green, Progress in Photovoltaics: Research and Applications. 4 (1996) 369-373.
[14] A. Blakers, Fuel and Energy Abstracts. 4 (1996) 279.
[15] K. Weber, A. Blakers, M. Stocks, M. Stuckings, A. Cuevas, A. Carr, T. Brammer, G. Matlakowski, IEEE Photovoltaic Specialists. 2 (1994) 1391-1393.
[16] A. Blakers, K. Weber, M. Stuckings, S. Armand, G. Matlakowski, A. Carr, M. Stocks, A. Cuevas, T. Brammer, Progress in Photovoltaics: Research and Applications. 3 (1995) 193-195.
[17] G. Zheng, W. Zhang, Z. Shi, M. Gross, A. Sproul, S. Wenham, M. Green, Solar Energy Materials and Solar Cells. 4 (1996) 231-238.
[18] S.A. Hadi, T. Milakovich, M.T. Bulsara, S. Saylan, M.S. Dahlem, E.A Fitzgerald, A. Nayfeh, IEEE Journal of Photovoltaics. 5 (2014) 425-431.
[19] K. A. Abade, F. J. Fonseca, R. D. Mansano, and P. Abade Jr., IEEE Photovoltaic Spec. Conf. (2000) 307-310.
[20] D. Yan, A. Cuevas, J. Stuckelberger, E.C. Wang, S.P. Phang, T.C. Kho, J.I. Michel, D. Macdonald, J. Bullock, Progress in Photovoltaics: Research and Applications. 31 (2023) 310-326.
[21] I. Lee, D.G. Lim, S.H. Lee, J. Yi, Surface and Coatings Technology. 137 (2001) 86-91.
[22] C. Ji, W. Liu, Y. Bao, X. Chen, G. Yang, B. Wei, F. Yang, X. Wang, Photonics. 9 (2022) 906.T. 23. Dzhafarov, InTech., 2013.
[23] G. Bauer, Annalen der Physik. 411 (1934) 434-464.
[24] S.E. Lee, S.W. Choi, J. Yi, Thin Solid Films. 276 (2000) 208-213.
[25] S.K. Dhungel, J. Yoo, K. Kim, S. Jung, S. Ghosh, J. Yi, Korean Phys Soc. 49 (2006) 885-889.
[26] R. Rathanasamy, G. Velu Kaliyannan, S. Sivaraj, A. Saminathan, B. Krishnan, D. Palanichamy, M.E. Uddin, Advances in Materials Science and Engineering, 2022.
[27] D.S Wuu, C.C. Lin, C.N. Chen, H.H. Lee, J.J. Huang, Thin Solid Films. 584 (2015) 248-252.
[28] N.I.I.M. Jamaluddin, M. Yahaya Bermakai, M.Z. Mohd Yusoff, Chalcogenide Lett. 19 (2022) 529-534.
[29] Y. Lee, D. Gong, N. Balaji, et al., Nanoscale Res Lett. 7 (2012) 50.
[30] R. Sharma, Turkish Journal of Physics. 42 (2020) 350–355.
[31] C. Becker, V. Preidel, D. Amkreutz, J. Haschke, B. Rech, Sol. Energ. Mat. Sol. C. 135 (2015) 2-7.
[32] X.J. Ma, T. Lin, Q.B. Chen, M.S. Zhang, International Journal of Nanomanufacturing. 9 (2013) 221
[33] M.Z. Pakhuruddin, J. Huang, J. Dore, S. Varlamov, IEEE Journal of Photovoltaics. 6 (2016) 852–859.
[34] N. Shanmugam, R. Pugazhendhi, R.E. Madurai, P. Kasiviswanathan, N. Das, Energies. 13 (2020) 2631.
[35] X. Wu, Applications of Titanium Dioxide Materials. IntechOpen. 2022